Journal of Organometallic Chemistry 693 (2008) 2971–2981

Contents lists available at ScienceDirect

Journal of Organometallic Chemistry

journal homepage: www.elsevier.com/locate/jorganchem

Self-assembly of *para*-OH functionalized ECE-metalated pincer complexes

Nilesh C. Mehendale [a], Martin Lutz [b], Anthony L. Spek [b], Robertus J.M. Klein Gebbink [a,*], Gerard van Koten [a,*]

[a] Chemical Biology and Organic Chemistry, Debye Institute for Nanomaterials Science, Faculty of Science, Utrecht University, Padualaan 8, 3584 CH Utrecht, The Netherlands
[b] Bijvoet Center for Biomolecular Research, Crystal and Structural Chemistry, Faculty of Science, Utrecht University, Padualaan 8, 3584 CH Utrecht, The Netherlands

ARTICLE INFO

Article history:
Received 7 April 2008
Received in revised form 9 June 2008
Accepted 12 June 2008
Available online 18 June 2008

Keywords:
Pincer complexes
Palladium
Platinum
Self-assembly
Hydrogen bonding
Siloxane

ABSTRACT

Various *para*-OH functionalized ECE–pincer metal complexes [MX(ECE–OH)L_n] (ECE–OH = [$C_6H_2(CH_2E)_2$-2,6-OH-4]$^-$, E = NMe_2, PPh_2 and SPh) were synthesized. The X-ray crystal structures of neutral [PdCl(SCS–OH)], [PdCl(NCN–OH)], and cationic [Pd(PCP–OH)(MeCN)](BF_4) are reported. The neutral halide complexes exhibit self-assembly to form polymeric chains *via* H-bonding involving the *para*-OH group as donors and the halide ligand on the metal as acceptors. Moreover, the halide ligand can be replaced by a monomeric aryloxy-O ligand leading to the formation of a covalently bonded dimer. The crystal structure of such a dimer derived from [PdI(NCN–OH)] is reported. Furthermore, these pincer–metal complexes were tethered through a carbamate linker to a siloxane functionality with the aim to be immobilized on a silica support. The crystal structure of a siloxane-functionalized [PtI(NCN–Z)] complex exemplifies how other H-bonding interactions not involving the metal–halide groupings can lead to polymeric networks as well.

1. Introduction

ECE–pincer metal complexes [MX(ECE–Z)L_n] (ECE–Z = [$C_6H_2(CH_2E)_2$-2,6-Z-4]$^-$, E = NMe_2, PPh_2 and SPh) with a *para*-functionality (Z) on the aromatic ring of the pincer anion are well known [1–9]. Electronic properties of the metal center can be tuned by inductive and mesomeric effects of this substituent [10]. Ample evidence has been gathered to show that catalytic properties of the pincer complex can be affected *via* the nature of the Z-substituent [2,11,12]. Furthermore, Z can be used to attach tethering groups which are suited to immobilize pincer–metal complexes to various supports, like polymers [3,13–15], silica [16–18], dendrimers [19,20], and bucky-balls [21], or peptides [6,22], and enzymes [23].

The Z-substituent can be introduced on the monoanionic ECE-ligand manifold prior to the binding of the metal, *i.e.* first the organic ligand is synthesized followed by a lithiation, *trans*-metalation, or oxidative addition reaction to attach the metal to the pincer ligand system. In many cases it could be demonstrated, however, that due to the stability of the pincer–metal grouping, it is possible to perform the *para*-functionalization directly on the ECE–pincer metal complex itself [5,24]. In the present study, we have taken advantage of the excellent stability and reactivity properties of ECE–pincer metal complexes and show that a *para*-OH substituent (Z = OH) on these complexes can be utilized for various purposes; *e.g.* for the formation of NCN–pincer metal polymers *via* non-covalent H-bonding as well as for the synthesis of siloxane-functionalized compounds which can be immobilized on silica.

Self-assembly of functionalized pincer–metal complexes controlled by H-bonding through a H-donor (Z-substituent) and a H-acceptor site (M–X) both in the solid-state and in solution has led to the finding of interesting polymers [25] and supramolecular structures [4,8,26–29]. For example, NCN–pincer Pt-complexes [PtCl(NCN–Z)] with Z = OH or C≡C–H form one-dimensional polymeric chains *via* intermolecular hydrogen bonds of the O–H···Cl [8] or C≡C–H···Cl [4,29] type, respectively, in the solid-state. These materials revealed reversible binding of SO_2 in the solid-state with retention of the polymeric structure [27,30]. Here, we have extended this concept to ECE–pincer Pd-complexes which are also known to be excellent catalysts for C–C and C–X bond formation reactions [5,11,15,20,22,31]. Interestingly, these ECE–pincer Pd-complexes likewise form polymeric structures *via* non-covalent H-bonding (**A**, Fig. 1). Moreover, we demonstrate how the zwitterionic species formed by HX elimination self-assemble to oligomeric structures via covalent M–O bonding (**B**, Fig. 1) [32].

2. Results and discussion

2.1. Synthesis of (ECE–OH)–pincer Pt- and Pd-complexes

Synthesis of the (ECE–OH)-pincer arene ligands **3–5** was initiated from *t*-butyldimethylsilyl-protected 3,5-bis(hydroxymethyl)phenol precursor **1** as shown in Scheme 1.

* Corresponding authors. Tel.: +31 30 2533120; fax: +31 30 2523615 (R.J.M. Klein Gebbink).
E-mail addresses: r.j.m.kleingebbink@uu.nl (R.J.M. Klein Gebbink), g.vankoten@uu.nl (G. van Koten).

0022-328X/$ - see front matter © 2008 Elsevier B.V. All rights reserved.
doi:10.1016/j.jorganchem.2008.06.016

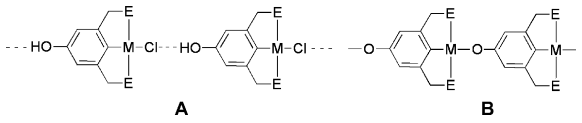

Fig. 1. Self-assembled polymers (A) *via* non-covalent H-bonding. Oligomers (B) *via* covalent M–O bonding.

This compound was synthesized from 5-hydroxy-isophthalic acid by a reported procedure in three steps [9,14,33]. Precursor **1** was converted to the bis-chloride **2** by a reaction with methane sulfonyl chloride followed by a simple treatment with suitable reagents ($LiPPh_2$, NaSPh, or Me_2NH) to afford the respective ECE–pincer arene ligand (E = PPh_2 **3**, SPh **4**, NMe_2 **5**). For the synthesis of (ECE–OH)–pincer Pd-complexes **6** and **7**, a direct bis-(*ortho*)-palladation route was used involving regioselective C–H activation using $[Pd(MeCN)_4](BF_4)_2$ as the palladating reagent (Scheme 2) [9].

In this reaction HBF_4 is generated as a co-product which, in a subsequent reaction, leads to complete deprotection of the 4-$OSiMe_2t$-Bu group. This avoids the deprotection step which otherwise would be necessary as is the case for the NCN–pincer complex. Further treatment of cationic (ECE–OH)–pincer Pd-complexes **6** and **7** with halide salts yielded the corresponding neutral ECE–pincer Pd–halide complexes **8** (X = Cl) and **9** (X = Cl (**9a**), Br (**9b**) and I (**9c**)).

The direct palladation route is not regioselective in the case of NCN–pincer ligands as both *ortho–ortho* and *ortho–para* palladation takes place [34]. Here, the use of an *ortho–ortho* directing group such as a trimethylsilyl one allows regioselective bis-(*ortho*)-palladation (Scheme 3) [35]. In this reaction, the *t*-$BuMe_2Si$ protection is not affected by the cyclopalladation reaction and has to be removed subsequently. The corresponding platinum complex **14a** was prepared by a published procedure (Scheme 3) [28,33].

2.2. Structures of [Pd(PCP–OH)(MeCN)]BF_4 (**6**), [PdCl(SCS–OH)] (**9a**), and [PdCl(NCN–OH)] (**13a**)

The cationic complex [Pd(PCP–OH)(MeCN)]BF_4 (**6**) was crystallized from its solution in acetonitrile. In the crystal structure there are two independent monomeric cations with the NCMe ligand coordinated *trans* to C_{ipso} (Fig. 2).

Like other pincer–metal complexes, the cation comprises a distorted square planar Pd center with an approximate C_2 symmetry axis along C_{ipso}–Pd–NCMe. The puckering of the five-membered chelate rings is in opposite direction with large torsion angles of −33.3(2)° for Pd(1)–P(11)–C(17)–C(12) and −38.1(2)° for Pd(1)–P(12)–C(120)–C(16). The 4-OH group acts as a hydrogen bond donor and the BF_4 anions act as acceptors. Each 4-OH group is hydrogen bonded to exactly one fluorine acceptor resulting in discrete monomeric species. Selected bond lengths are reported in Table 1.

[PdCl(SCS–OH)] (**9a**) was found to be less soluble in most organic solvents except in DMSO, from which single crystals suitable for X-ray diffraction could be obtained. The molecular structure shows the common structural features for SCS–pincer Pd-complexes, such as a four-coordinate Pd center with square planar geometry and an approximate C_2 symmetry axis along C_{ipso}–Pd–Cl (Fig. 3a).

The five-membered palladacycles are puckered in opposite directions with torsion angles Pd(1)–S(1)–C(7)–C(2) and Pd(1)–

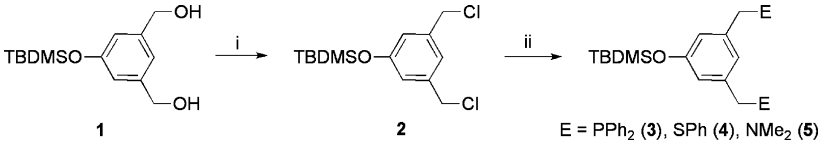

Scheme 1. Synthesis of (ECE–OH)–pincer arene ligands; (i) $MeSO_2Cl$, NEt_3, CH_2Cl_2, RT, 16 h; (ii) (a) $LiPPh_2$, THF; (b) NaSPh, THF; or (c) $HNMe_2$, NEt_3, THF.

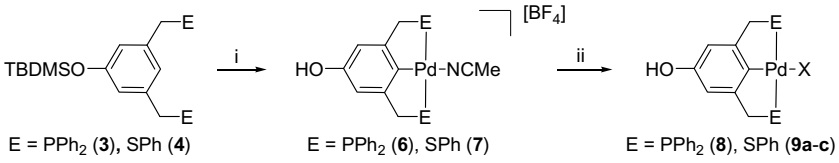

Scheme 2. PCP– and SCS–pincer Pd-complexes by a direct bis-(*ortho*)-palladation route; (i) $[Pd(MeCN)_4](BF_4)_2$, MeCN; (ii) NaX, CH_2Cl_2/H_2O (**8**, **9a**: X = Cl; **9b**: X = Br; **9c**: X = I).

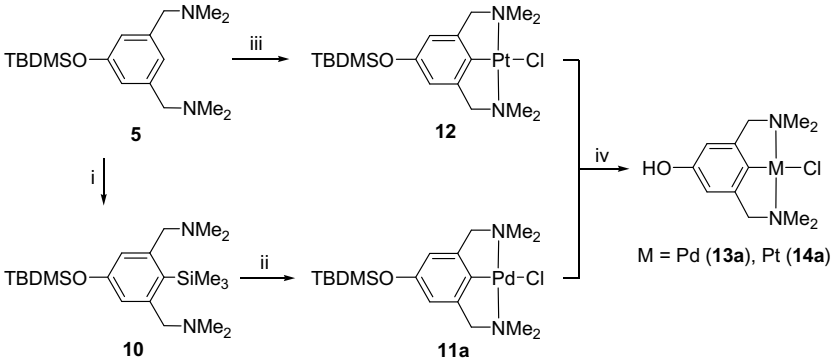

Scheme 3. NCN–pincer Pd and Pt-complexes by the transmetalation route; (i) (a) *n*BuLi, −78 °C, hexane, (b) Me_3SiCl, 0 °C,THF; (ii) (a) $Pd(OAc)_2$, MeOH, (b) LiCl, MeOH; (iii) (a) *n*BuLi, −78 °C, hexane, (b) $[PtCl_2(Me_2S)_2]$, ether; (iv) (a) nBu_4NF, THF, (b) 0.2 M HCl.

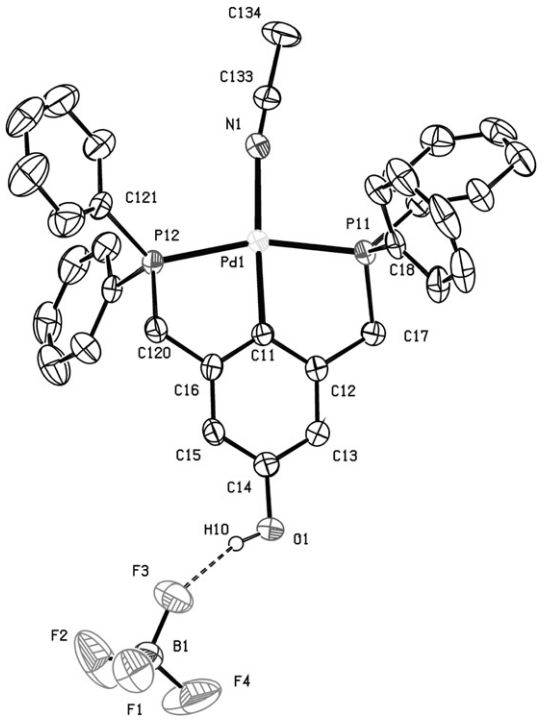

Fig. 2. Displacement ellipsoid plot of one of the two independent molecules of cationic PCP–pincer Pd(II)-complex **6** in the crystal, drawn at the 50% probability level. C–H hydrogen atoms are omitted for clarity.

S(2)–C(14)–C(6) of 10.25(15)° and 15.95(15)°, respectively. The phenyl ring on S(2) is orientated almost parallel to the C_2 axis, whereas that on S(1) is perpendicular to it. The crystal structure reveals some more unique features. The molecular units form non-covalently bonded polymers in the direction of the crystallographic *a,b*-diagonal involving intermolecular H-bonding between the OH group as a H-donor and the chloride ligand as a H-acceptor (Fig. 3b). The O–H bond length is 0.79(3) Å and the Cl···H distance is 2.31(3) Å, while the O–H···Cl angle amounts to 178(3)°. Amongst the complexes **9a**, **13a**, and **14a**, it is observed that **9a** has the shortest Cl···H distance and the largest O–H···Cl angle, indicating the strongest H-bonding interaction. Selected bond lengths and angles are reported in Table 1. In the crystal, two parallel chains run in the same direction, while due to the centrosymmetric space group there are also two parallel chains running in opposite direction cancelling the directionality as a whole (not shown).

Finally, single crystals of complex [PdCl(NCN–OH)] (**13a**) suitable for X-ray crystallography were obtained by slow evaporation of its methanol solution. Interestingly, **13a** is isostructural with the corresponding platinum complex [PtCl(NCN–OH)] (**14a**) [8]. A molecular plot of **13a** is given in Fig. 4. Torsion angles Pd(1)–N(1)–C(7)–C(2) and Pd(1)–N(2)–C(10)–C(6) of −28.5(2)° and −29.5(2)°, respectively, are found with puckering of the five-membered palladacycles in opposite directions. Crystal packing and the hydrogen bonding interactions, which form a one-dimensional chain, have already been described for the isostructural platinum complex [8].

2.3. IR studies

The O–H vibration of various neutral [PdX(SCS–OH)] (**9**) type complexes with different halides reveals that the O–H stretching frequency increases from X = Cl to Br to I (3213, 3269, 3305 cm^{-1}, respectively) in the solid-state (Table 2). In the series [PdCl(ECE–OH)] (E = N (**13a**), P (**8**) and S (**9a**)), the OH stretching frequencies of the NCN– (3252 cm^{-1}) and PCP– (3254 cm^{-1}) pincer complexes are similar, whereas, the SCS–pincer complex has a lower value (3213 cm^{-1}). This corroborates the findings from X-ray crystallography, in that the H-bonding interaction between [PdCl(SCS–OH)] complexes is stronger than for the other two complexes. This trend is also reflected in the solubility of these complexes in common organic solvents like dichloromethane. SCS–pincer complex **9a** (X = Cl) has the lowest solubility, which improves when the halide is changed to Br (**9b**) or I (**9c**). Similarly, PCP– and NCN–pincer complexes have a better solubility than the SCS–pincer ones.

A similar trend for the O–H vibration is observed for the [PtX(NCN–OH)] complexes (X = Cl (**14a**) and I (**14b**)). The OH stretching frequency in the solid-state increases from **14a** to **14b**; and **14b** also has the higher solubility in organic solvents compared to **14a**.

The cationic PCP– and SCS–pincer Pd-complexes **6** and **7** have similar O–H stretching frequencies at 3431 and 3436 cm^{-1}, respectively. For the [Pd(PCP–OH)(NCMe)] cation [**6**]$^+$, H-bonding exists with the BF_4 anion as established in the solid-state (Fig. 2). Most likely, complex **7** shows a similar H-bonding with the anion. Both complexes can be seen either as a cationic complex to which the BF_4 anion is bonded *via* H-bonding (Structure **C**, Fig. 5) or as a zwitterionic complex having an anionic O-grouping H-bonded to $H(BF_4)$, while the cationic site is blocked by coordination of a neutral acetonitrile ligand (Structure **D**). This prevents polymeric chain formation in these complexes and thereby increases their solubility. The higher O–H stretching frequencies of both cationic complexes **6** and **7** (3431 and 3436 cm^{-1}, respectively) compared to those of neutral complexes **8** and **9**, indicate a weak H-bonding in both **6** and **7** and consequently point to the structural moiety **C** in Fig. 5.

2.4. Synthesis of dimer *15*

In general, deprotection of the TBDMS-group from the *para*-OTBDMS grouping in NCN–pincer Pd-complex **11** involves treatment of the pincer metal complex with tetrabutylammonium fluoride (TBAF) in THF, followed by an acidic work-up [14,33]. The

Table 1
Selected bond lengths (Å) and angles (°) of **6**, **9a**, **13a** and **14a**

	[Pd(PCP–OH)(NCMe)](BF_4) (**6**)[a]	[PdCl(SCS–OH)] (**9a**)	[PdCl(NCN–OH)] (**13a**)	[PtCl(NCN–OH)] (**14a**) [8]
M–Cl	2.082(3) (Pd–N)	2.4095(5)	2.4420(6)	2.433(2)
M–C	2.021(3)	1.9831(18)	1.928(2)	1.915(9)
M–E	2.2994(8), 2.3098(7)	2.2861(5), 2.3140(5)	2.114(2), 2.111(2)	2.083(8), 2.094(8)
O–H	0.86	0.79(3)	0.72(3)	0.84(14)
Cl···H		2.31(3)	2.42(3)	2.32(13)
O–Cl		3.1040(18)	3.119(2)	3.127(8)
O–C	1.378(4)	1.368(2)	1.375(3)	1.389(12)
O–H–Cl		178(3)	165(4)	162(15)
M–Cl–H		106.5(7)	119.0(7)	115(4)

[a] Only one of two independent molecules is considered.

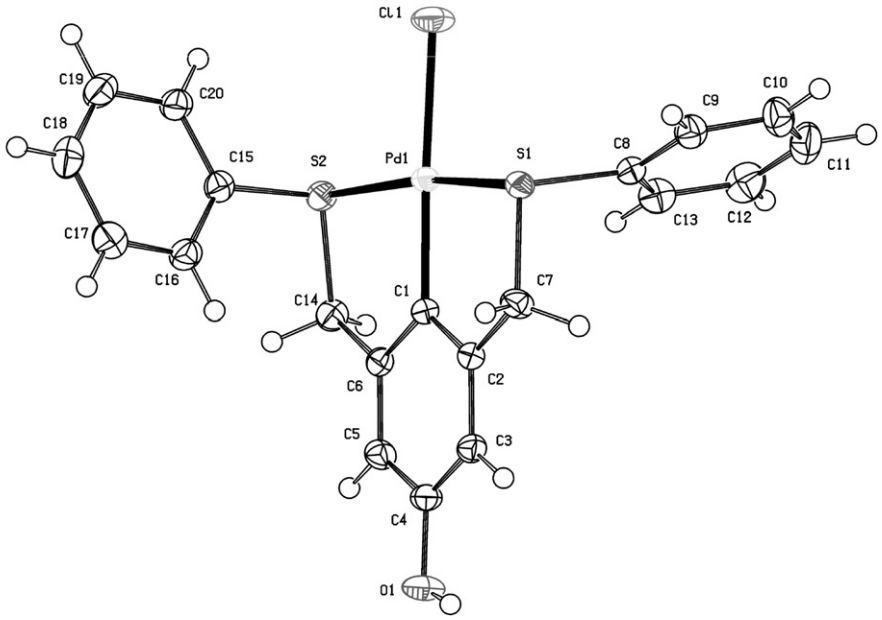

Fig. 3a. Displacement ellipsoid plot of [PdCl(SCS–OH)] (**9a**) in the crystal, drawn at the 50% probability level.

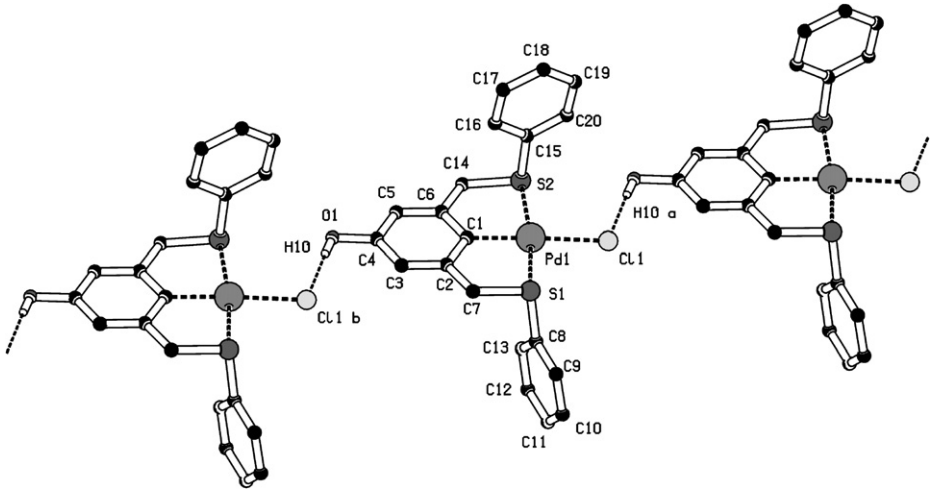

Fig. 3b. Hydrogen bonding interactions forming a one-dimensional chain in the crystal structure of [PdCl(SCS–OH)] (**9a**). Projection along the crystallographic *c*-axis. C–H hydrogen atoms are omitted for clarity. Symmetry operations (i) $x + 0.5$, $y + 0.5$, z; (ii) $x - 0.5$, $y - 0.5$, z.

yields for these reactions are moderate (about 50%). In the case of the NCN–pincer palladium complex **11b** more detailed information about the possible reason for this observation was obtained. Deprotection of [PdI(NCN–OSi*t*-BuMe_2)] (**11b**) was carried out by reaction with a 1 M solution of TBAF in THF. A subsequent non-acidic work-up was used to avoid halide scrambling (Scheme 4).

The yellow product obtained after work-up was found to be less soluble than the silyl-protected analog in solvents like methanol and dichloromethane. The ^{1}H NMR spectrum of a solution of the yellow product in $(CD_3)_2SO$ showed only one set of broad peaks. However, the ^{1}H NMR spectrum of a CD_2Cl_2 solution revealed two distinct sets of signals for the *N*-methyl, benzyl and aromatic hydrogens, indicating the presence of two non-equivalent pincer moieties. On the basis of ^{1}H and ^{13}C NMR data and elemental analysis, the product was formulated as dimer **15** (see Scheme 4). Further structural analysis confirmed the dimeric nature of **15** in the solid-state.

2.5. X-ray crystal structure of *15*

Crystals of **15** · MeOH suitable for X-ray structure determination were obtained from a saturated solution in methanol. The molecular picture shows a unique structure consisting of a Pd-cation $[Pd(NCN–OH)]^+$ bonded *via* a Pd–O bond to a phenolate-anion $[PdI(NCN–O)]^-$ (Fig. 6). Moreover, in a distinct manner one molecule of methanol per dimeric unit is bonded to the two kinds of O-atoms present, *i.e.* to the phenoxy-O and the phenol-O, respectively. Selected bond lengths and bond angles are reported in Table 3.

The Pd(2)–O(1)–C(41) angle is 117.1(3)° while the O(1)–C(41) bond length (1.338(4) Å) of the $[PdI(NCN–O)]^-$ phenolate-anion is shorter than the O(2)–C(42) (1.381(5) Å) bond in the $[Pd(NCN–OH)]^+$ cation. In fact, for all monomeric [MX(ECE–OH)] *para*-OH pincer complexes reported so far, the O–C bond length falls in the range of 1.36–1.38 Å (Table 1), which is considerably longer

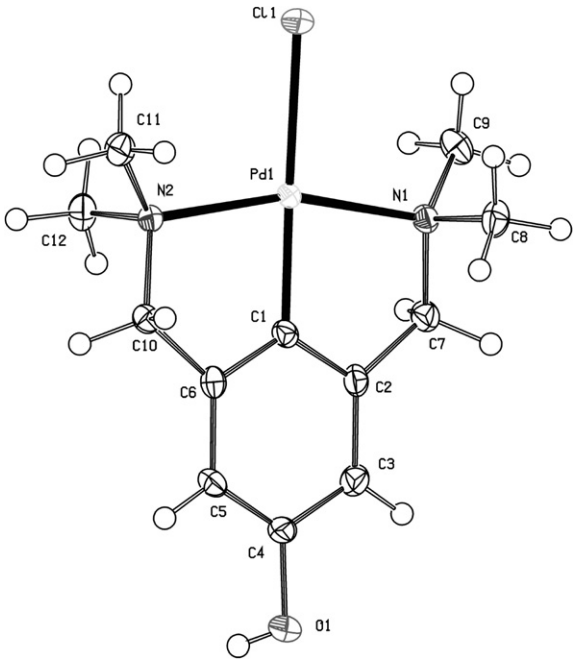

Fig. 4. Displacement ellipsoid plot of [PdCl(NCN–OH)] (**13a**) in the crystal, drawn at the 50% probability level.

Table 2
O–H stretching vibration of [MX(ECE–OH)L_n] pincer metal complexes in the solid-state

Compound	O–H vibration (cm^{-1})
[Pd(PCP–OH)(NCMe)](BF_4) (**6**)	3431
[Pd(SCS–OH)(NCMe)](BF_4) (**7**)	3436
[PdCl(PCP–OH)] (**8**)	3254
[PdCl(SCS–OH)] (**9a**)	3213
[PdBr(SCS–OH)] (**9b**)	3269
[PdI(SCS–OH)] (**9c**)	3305
PdCl(NCN–OH) (**13a**)	3252
PtCl(NCN–OH) (**14a**)	3280
PtI(NCN–OH) (**14b**)	3335

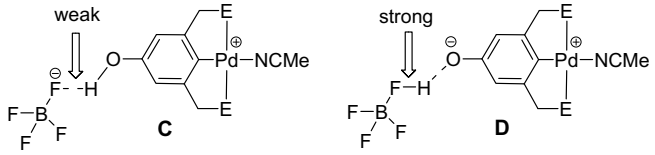

Fig. 5. Two possible binding motifs of ECE–OH–pincer palladium cationic complexes.

than the O–C bond length (1.338(4) Å) in the phenolate-anion itself. These results are comparable to the results from the crystal structure of the parent [Pd(OPh)NCN] complex published earlier, which contains a phenoxy anion as the fourth ligand [36]. It is interesting to note that in the NCN-palladium dimer **15** one molecule of methanol is H-bonded to the phenoxy-O anion while the phenol-OH of the same dimer is also involved in H-bonding with another methanol molecule. Each methanol molecule is involved in two H-bonds. It acts as a H-bond donor to the phenoxy-O anion of one dimer and as a H-bond acceptor to the phenol grouping of another dimer, thereby forming a network structure. In aryloxypalladium and platinum chemistry, these binding motifs are a common feature, *e.g.* they have been found in [Pt(Me)(OPh)(bpy)] · HOPh [37], [Pd($OCH(CF_3)_2$)(OPh)(bpy)] · HOPh [38], [Pt(OPh)(NCN)] · HOPh, and [Pt(catecholate)(NCN)] [36], respectively.

Reaction of dimer **15** (yellow) with ammonium iodide resulted in the formation of monomeric [PdI(NCN–OH)] (**13b**; colorless, Scheme 4), which was confirmed by ^{1}H NMR spectroscopic and elemental analytic data, as well as by comparison of these data with those of an authentic sample. Thus, dimer formation is a reversible process and can be achieved by treatment of the dimer with NH_4I which provides HI to form monomer **13b**. In fact, by increasing the pH of a solution of **13b** in MeOH, HX can be removed from [MX(NCN–OH)] to form the dimer **15**, whereas, by decreasing the pH, this dimer can be transformed back into its monomeric form. Dimerization is also a first step in the process of organometallic polymer formation *via* a direct metal–oxygen bond (**B**, Fig. 1). Thus it is possible to form polymeric chains by removal of the phenolic proton from [PdX(NCN–OH)] by a base, with the resulting phenoxide then replacing the halide from palladium of the next molecule to form a Pd–O bond. This process is currently under investigation as it may give rise to the formation of unique organometallic polymers in which the organometal phenoxide is the repetitive unit.

2.6. Synthesis of siloxane-functionalized ECE–pincer complexes (*16*–*19*)

The current interest in the catalytic activity of ECE–pincer Pd-complexes in C–C and C–X cross-coupling reactions [5,11,15,20,22,31] combined with the possibility to recycle these complexes *via* the *para*-OH functionality make the present complexes highly interesting. Immobilization of these complexes on silica has a twofold advantage; separation of the catalyst from the product can be achieved as well as recycling. One of the major problems in heterogenizing homogeneous catalysts on inorganic supports like silica is the determination of the exact catalyst structure on the support; *i.e.* whether the molecular structure has been retained after immobilization and whether the catalytic center is still accessible. In this respect, we decided to use the *para*-OH grouping of the present complexes for the synthesis of modified pincer–metal complexes tethered with a *para*-siloxane group suitable for immobilization.

The triethoxysilane tethered complexes **16**–**19** were prepared by refluxing the respective (ECE–OH)–pincer metal complexes with triethoxysilylpropyl isocyanate in the presence of a combination of two Lewis bases; 0.05 equiv. of 4-(dimethylamino)pyridine (DMAP) and 1.1 equiv. of NEt_3. The siloxane-functionalized complexes were isolated in about 90% yield (Scheme 5). Prior to the reaction of [PdCl(SCS–OH)] **9a** with triethoxysilylpropyl isocyanate, the chloride was exchanged to bromide (**9b**) in order to first increase the solubility of the SCS–pincer palladium complex. It appeared that this approach facilitated a faster and more complete

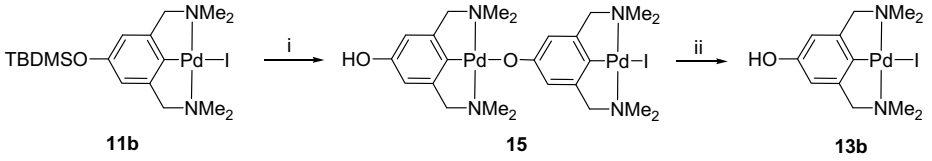

Scheme 4. Deprotection of **11b** and formation of dinuclear **15**; (i) nBu$_4$NF, THF. Reaction of **15** with NH_4I (ii) affording mononuclear [PdI(NCN–OH)] **13b**.

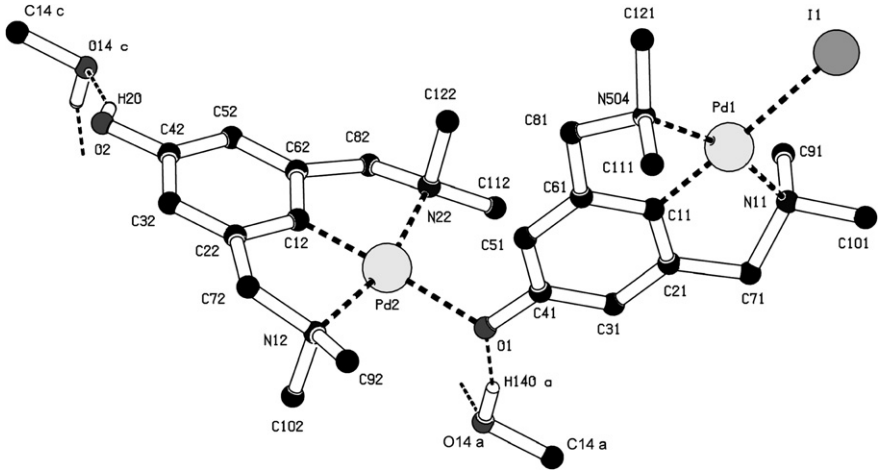

Fig. 6. Molecular geometry of dimer **15** · MeOH; hydrogens, except those involved in H-bonding, are omitted for clarity.

Table 3
Selected bond lengths (Å) and angles (°) of dinuclear complex **15** · MeOH

Pd(1)–I(1)	2.7373(4)
Pd(2)–O(1)	2.159(3)
Pd(1)–C(11)	1.930(4)
Pd(2)–C(12)	1.914(4)
O(1)–C(41)	1.338(4)
O(2)–C(42)	1.381(5)
Pd(2)–O(1)–C(41)	117.1(3)

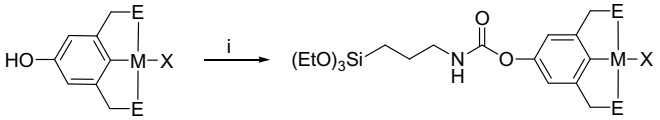

M = Pd: **16**, E = NMe_2, X = Cl; **18**, E = PPh_2, X = Cl;
19, E = SPh, X = Br
M = Pt: **17**, E = NMe_2, X = I

Scheme 5. Pincer metal complexes functionalized with a triethoxysilane grouping suitable for coupling to silica; (i) 1.1 equiv. $(EtO)_3Si(CH_2)_3NCO$, 1.1 equiv. NEt_3, 0.05 equiv. DMAP, CH_2Cl_2, reflux.

conversion to **19**. For the same reason, the chloride of [PtCl(NCN–OH)] **14a** was first exchanged to iodide (**14b**). Complexes **16**–**19** all comprise a trialkoxysilane and an organometallic fragment covalently connected through a propylcarbamate linker. Again, the absence of H-bond forming *para*-OH groups and the presence of a non-polar tail including a silyl grouping increased the solubility of these complexes considerably. They are even soluble in non-polar solvents such as benzene or toluene, which allowed grafting of these complexes on silica in these solvents [39]. Details on the grafting procedures and on the use of modified silica's in catalysis were reported by our group [16,17].

2.7. X-ray crystal structure of **17**

The molecular structure of the NCN–pincer Pt-complex **17** in the solid-state was determined by single crystal X-ray crystallography (Fig. 7).

The platinum atom has a square planar coordination environment. The phenyl grouping of the NCN–pincer ligand makes a dihedral angle of 14.95(16)° with respect to the platinum coordination plane. The two five-membered Pt–C–C–C–N chelate rings are puckered in such a way, that a local C_2 symmetry is generated. The torsion angles Pt(1)–N(1)–C(7)–C(2) and Pt(1)–N(2)–C(8)–C(6) are −33.9(4)° and −32.4(4)°, respectively. The carbamate group (*i.e.* the NC(=O)O plane) is positioned almost perpendicularly to the phenyl ring with a dihedral angle of 84.9(2)°. The C_3-alkyl chain with the triethoxysilyl end group is in an extended conformation. Selected bond lengths and angles are reported in Table 4.

An interesting structural feature is the way the carbamate groupings are intermolecularly connected by non-covalent H-bonding. In contrast with previous structures (as in *e.g.* **14a**) this

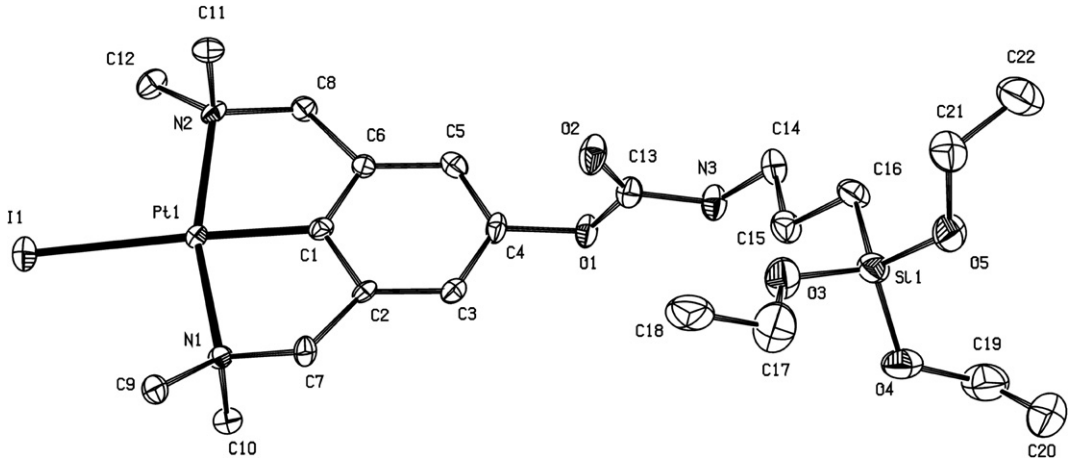

Fig. 7. Displacement ellipsoid plot of the NCN–pincer Pt-complex **17**, drawn at the 50% probability level. Hydrogen atoms have been omitted for clarity.

Table 4
Selected bond lengths (Å) and angles (°) for **17**

Bond lengths		Bond angles	
Pt1–C1	1.940(4)	C1–Pt1–N1	81.47(17)
Pt1–N1	2.104(4)	C1–Pt1–N2	80.91(16)
Pt1–N2	2.094(4)	N2–Pt1–N1	162.36(14)
Pt1–I1	2.7013(4)	C1–Pt1–I1	175.96(13)
O1–C13	1.365(6)	N2–Pt1–I1	99.98(10)
O2–C13	1.214(6)	N1–Pt1–I1	97.65(10)
N3–C13	1.331(6)	C4–O1–C13	115.8(3)
		O1–C13–N3	110.5(4)
		C13–N3–C14	121.1(4)

is not involving the Pt–Cl grouping, but occurs through the hydrogen of the NH-grouping of one molecule with the C = O grouping of a neighboring molecule [H(3)···O(2)^{i} 2.21 Å, N(3)···O(2)^{i} 2.955(5) Å, N(3)–H(3)···O(2)^{i} 143°, symmetry operation (i) x, $0.5 - y$, $z - 0.5$]. By this non-covalent hydrogen bonding, an infinite chain is formed in the direction of the crystallographic *c*-axis (Fig. 8).

As a result, all NCN–pincer platinum units are arranged at one site with the $Si(OEt)_3$ groups residing on the opposite site, which creates a kind of model mimicking possible surface arrangements of the NCN–pincer platinum groupings upon immobilization of **17** on a silica surface (see axial view in Fig. 8).

3. Conclusions

The possibility to induce selective H-bonding between organometallic complexes is of prime interest in the field of crystal engineering [40]. It can be used to direct formation of aggregates with special shapes (rings, chains, polymers, etc.) and distinct stereochemistries. These materials could have various interesting applications such as conducting polymers, as LED's, or as materials with NLO properties.

The [MX(ECE–OH)] complexes are bifunctional molecules, which have unique H-bonding properties *via* a combination of the *para*-OH and M–halide entities present in one building block. Ample evidence has been collected now that in the protonated form, they afford self-assembled, non-covalent polymeric chains [27,30]. Moreover, *via* selective deprotonation followed by halide-phenoxy anion exchange, dimeric structures are accessible. This deprotonation approach with ultimate HX elimination and removal provides a possibility to form oligomers or even polymers through mutual intermolecular M–O bond formation. Consequently, these complexes can be interesting building blocks to form novel organometallic polymers.

In addition, the excellent stability of these [MX(ECE–OH)] complexes under severe reaction conditions (*e.g.* highly acidic and electrophilic or highly basic and nucleophilic conditions) allows their direct *para*-functionalization with siloxane substituted tethers providing [MX(ECE–Z)] complexes which are potential candidates for the synthesis of recyclable, immobilized homogeneous catalysts [3,13,15,17,18]. At the same time this approach also allows for the introduction of other H-bonding moieties, not including the M–Cl grouping, like, *e.g.*, carbamates. This approach could be of interest in the field of self-assembling and self-organizing polymers [25].

4. Experimental

4.1. General

Synthetic procedures were conducted under a dry nitrogen atmosphere using standard Schlenk techniques. Solvents were dried over appropriate materials and distilled prior to use. Moreover, for the synthesis of PCP–pincer ligands and complexes, solvents were degassed prior to use. Reagents were obtained from commercial sources and were used without further purification. Siloxane materials were stored under nitrogen atmosphere. ^{1}H (200.1 and 300.1 MHz), $^{13}C\{^{1}H\}$ (50.3 and 75.5 MHz) and $^{31}P\{^{1}H\}$ (81 MHz) NMR spectra were recorded at room temperature on either Varian Mercury 200 or Varian Inova 300 spectrometers. FT-IR spectra were recorded using a Mattson Instruments Galaxy Series FTIR 5000 spectrometer. Microanalyses were obtained from H. Kolbe Mikroanalytisches Laboratorium, Mülheim an der Ruhr, Germany.

Compounds **1**–**4** were synthesized following literature procedures [7,9,41]. 3,5-Bis[(dimethylamino)methyl]-4-(trimethylsilyl)phenyl *tert*-butyldimethylsilyl ether (**10**) [9,14,33] and (2,6-bis[(dimethylamino)methyl]-4-(hydroxy)phenyl)platinum(II) iodide (**14b**) [8,28] were prepared as described previously.

4.2. Synthesis of $[Pd\{C_6H_2(CH_2PPh_2)_2\text{-}2,6\text{-}(OH)\text{-}4\}(MeCN)]BF_4$ (**6**)

$[PdCl_2(MeCN)_2]$ (0.33 g, 1.26 mmol) was dissolved in refluxing acetonitrile (30 mL). $AgBF_4$ (0.49 g, 2.52 mmol) dissolved in acetonitrile (10 mL) was added to this solution, upon which immediate precipitation of AgCl occurred. The reaction mixture was stirred for another hour. The precipitate formed was allowed to settle, after which the supernatant was decanted into a solution of **3** (0.76 g, 1.26 mmol) in warm acetonitrile (30 mL). The resulting orange mixture was stirred at 50 °C for 16 h to yield a yellowish colored

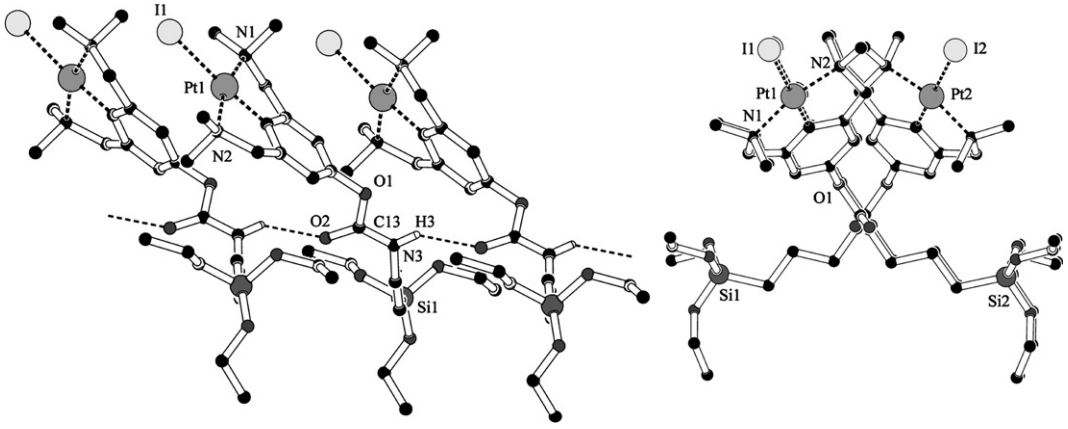

Fig. 8. H-bonding in the NCN–pincer Pt-complex **17**; lateral view (left) and axial view (right) showing the regular arrangement of siloxy-groups. (Hydrogen atoms, except those involved in H-bonding, have been omitted for clarity.)

turbid mixture. The mixture was allowed to settle and the supernatant was filtered off, all volatiles were evaporated, and the resulting light yellow solid was redissolved in a dichloromethane/acetonitrile mixture (10 mL/3 mL) and this solution was filtered again. After evaporation of all volatiles, the product was washed with diethyl ether and dried *in vacuo*. A light yellow powder **6** (0.85 g, 1.17 mmol) was obtained in 94% yield. ^{1}H NMR (300.1 MHz, CD_3CN, 25 °C): δ = 1.96 (s, 3H, C*H*$_3$CN); 3.99 (vt, $^2J_{H,P}$ = 4.7 Hz, 4H, C*H*$_2$P); 6.67 (s, 2H, Ar*H*); 7.5–7.6 (m, 12H, Ph*H*); 7.7–7.75 (m, 8H, Ph*H*). ^{13}C NMR (75.5 MHz, CD_3CN, 25 °C): δ = 41.12 (vt, $^1J_{C,P}$ = 15.3 Hz, *C*H$_2$P); 112.63 (vt, $^3J_{C,P}$ = 12 Hz, *m*-C Ar), 130.31 (vt, $^3J_{C,P}$ = 4.9 Hz, *m*-C Ph), 131.39 (vt, $^1J_{C,P}$ = 23.1 Hz *ipso*-C Ph), 132.64 (*p*-C Ph), 133.76 (vt, $^2J_{C,P}$ = 7.1 Hz, *o*-C Ph), 144.86 (*ipso*-C Ar), 149.83 (vt, $^2J_{C,P}$ = 10.3 Hz, *o*-C Ar), 157.71 (*p*-C Ar). ^{31}P NMR (81 MHz, CD_3CN, 25 °C): δ = 41.9. IR (ATR): $\tilde{\nu}$ (cm^{-1}) = 3430, 3059, 2943, 2893, 2323, 2293, 1591, 1568, 1484, 1455, 1435, 1305, 1069, 742. Anal. Calc. for $C_{34}H_{30}BF_4NOP_2Pd$ (723.78): C, 56.42; H, 4.18; N, 1.94; P, 8.56. Found: C, 56.48; H, 4.33; N, 1.94; P, 8.52%.

4.3. Synthesis of [Pd{$C_6H_2(CH_2SPh)_2$-2,6-(OH)-4}(MeCN)]BF_4 (**7**)

A similar procedure was followed as for the synthesis of **6**. Using **4** (1.1 g, 2.43 mmol), **7** was obtained as an orange colored powder in 84% yield. ^{1}H NMR (300.1 MHz, CD_3CN, 25 °C): δ = 4.63 (bs, 4H, C*H*$_2$S); 6.56 (s, 2H, Ar*H*); 7.46–7.54 (m, 6H, Ph*H*); 7.80-7.84 (m, 4H, Ph*H*). ^{13}C NMR (75.5 MHz, CD_3CN, 25 °C): δ = 50.72 (*C*H$_2$S); 111.45 (*m*-C Ar), 131.09 (*o*-C Ph), 131.75 (*p*-C Ph), 132.02 (*ipso*-C Ph), 132.57 (*m*-C Ph), 146.84 (*ipso*-C Ar), 152.34 (*o*-C Ar), 156.40 (*p*-C Ar). IR (ATR): $\tilde{\nu}$ (cm^{-1}) = 3437, 3059, 2937, 2288, 1593, 1576, 1473, 1441, 1431, 1312, 1053, 743. Anal. Calc. for $C_{22}H_{20}BF_4NOPdS_2$ (571.76): C, 46.21; H, 3.53; N, 2.45; S, 11.22. Found: C, 46.12; H, 3.64, N, 2.38; S, 11.27%.

4.4. Synthesis of [PdCl{$C_6H_2(CH_2PPh_2)_2$-2,6-(OH)-4}] (**8**)

To an orange solution of **6** (0.2 g, 0.276 mmol) in acetonitrile (3 mL), a solution of NaCl (0.24 g, 4.1 mmol) in demineralized water (5 mL) was added. A turbid orange colored mixture was obtained, stirred for another 16 h at ambient temperature, and then concentrated to dryness. The resulting residue was dissolved in dichloromethane and washed with excess water, dried over $MgSO_4$, filtered and volatiles evaporated *in vacuo*. A yellow colored **8** was obtained in quantitative yield. ^{1}H NMR (300 MHz, CD_3CN + $(CD_3)_2SO$, 25 °C): δ = 3.96 (vt, $^2J_{H,P}$ = 4.8 Hz, 4H, C*H*$_2$P); 6.62 (s, 2H, Ar*H*); 7.43–7.47 (m, 12H, Ph*H*); 7.84–7.90 (m, 8H, Ph*H*); 8.86 (s, 1H, O*H*). ^{13}C NMR (75.5 MHz, CD_3CN + $(CD_3)_2SO$, 25 °C): δ = 42.22 (vt, $^1J_{C,P}$ = 15 Hz, *C*H$_2$P); 111.93 (vt, $^3J_{C,P}$ = 11.9 Hz, *m*-C Ar), 129.67 (vt, $^3J_{C,P}$ = 4.9 Hz, *m*-C Ph), 131.68 (*p*-C Ph), 133.34 (vt, $^1J_{C,P}$ = 21 Hz *ipso*-C Ph), 133.76 (vt, $^2J_{C,P}$ = 7 Hz, *o*-C Ph), 148.64 (*ipso*-C Ar), 149.45 (vt, $^2J_{C,P}$ = 11 Hz, *o*-C Ar), 157.28 (*p*-C Ar). ^{31}P NMR (81 MHz, CD_3CN + $(CD_3)_2SO$, 25 °C): δ = 39.04. IR (ATR): $\tilde{\nu}$ (cm^{-1}) = 3254, 3051, 1590, 1564, 1482, 1434, 1417, 1304, 742, 692. Anal. Calc. for $C_{32}H_{27}ClOP_2Pd$ (631.38): C, 60.87; H, 4.31; P, 9.81. Found: C, 60.73; H, 4.38; P, 9.76%.

4.5. Synthesis of [PdX{$C_6H_2(CH_2SPh)_2$-2,6-(OH)-4}] (**9**)

A solution of **7** (0.5 g, 0.875 mmol) in acetonitrile (20 mL) was treated with a solution of NaX (0.5 g, 8.7 mmol) in distilled water (5 mL), which resulted in the formation of a turbid orange colored mixture. After stirring at ambient temperature for 2 h, the reaction mixture was concentrated to remove volatiles. The residue obtained was washed with excess water leaving an orange colored product which was dried *in vacuo*. Compound **9** was obtained in almost quantitative yield. ^{1}H NMR (300 MHz, $(CD_3)_2SO$, 25 °C): δ = 4.67 (s, 4H, C*H*$_2$S); 6.48 (s, 2H, Ar*H*); 7.43–7.48 (m, 6H, Ph*H*); 7.82–7.85 (m, 4H, Ph*H*); 9.25 (s, 1H, O*H*). ^{13}C NMR (75.5 MHz, $(CD_3)_2SO$, 25 °C): δ = 49.80 (*C*H$_2$S); 109.68 (*m*-C Ar), 129.39 (*p*-C Ph), 129.54 (*o*-C Ph), 130.69 (*m*-C Ph), 132.41 (*ipso*-C Ph), 149.69 (*ipso*-C Ar), 150.25 (*o*-C Ar), 154.82 (*p*-C Ar). IR (ATR): $\tilde{\nu}$ (cm^{-1}) = 3213, 3043, 2906, 1591, 1574, 1471, 1439, 1421, 1314, 741. Anal. Calc. for $C_{20}H_{17}BrOPdS_2$ (9b, 523.8): C, 45.86; H, 3.27; S, 12.24. Found: C, 45.95; H, 3.19; S, 12.24%.

4.6. Synthesis of [PdCl{$C_6H_2(CH_2NMe_2)_2$-2,6-(t-BuMe$_2$SiO)-4}] (**11a**)

$Pd(OAc)_2$ (0.569 g, 2.54 mmol) was added to a solution of **10** (1 g, 2.54 mmol) in methanol (25 mL). The resulting red-brown colored, clear solution was stirred at room temperature for 2 h after which an excess of LiCl (0.5 g, 10 mmol) was added and stirring was continued for 1 h. After evaporation of volatiles, the resulting green colored solid was dissolved in dichloromethane. The solution was filtered over a packed Celite column. The filtrate was concentrated and a solid was precipitated by addition of pentane. Centrifugation followed by drying of the precipitate in vacuum led to the isolation of **11a** as a colorless solid in 89% yield. ^{1}H NMR (300 MHz, $CDCl_3$, 25 °C): δ = 0.16 (s, 6H, SiMe$_2$); 0.96 (s, 9H, Si*t*-Bu); 2.92 (s, 12H, NC*H*$_3$); 3.92 (s, 4H, C*H*$_2$N); 6.30 (s, 2H, Ar*H*). ^{13}C NMR (50 MHz, $CDCl_3$, 25 °C): δ = −4.19 (SiCH$_3$); 18.33 (SiC(CH$_3$)$_3$); 25.88 (SiC(*C*H$_3$)$_3$); 53.33 (NCH$_3$); 74.86 (*C*H$_2$N); 111.97, 145.56, 147.51, 153.53 (Ar*C*). Anal. Calc. for $C_{18}H_{33}ClN_2OPdSi$ (463.43): C, 46.65; H, 7.18; N, 6.04. Found: C, 46.78; H, 7.04; N, 5.93%.

4.7. Synthesis of [PdCl{$C_6H_2(CH_2NMe_2)_2$-2,6-(OH)-4}] (**13a**)

A solution of **11a** (1 g, 2.16 mmol) in THF (25 mL) was treated with a solution of tetrabutylammonium fluoride in THF (1 M, 2.5 mL, 2.5 mmol), which formed a clear red-brown colored solution. After stirring for 2 h at ambient temperature, the reaction mixture was concentrated to a quarter of its volume and then treated with 0.2 M HCl (12.5 mL), which caused turbidity. Stirring was continued for 1 h. The precipitate was then filtered and washed with water (25 mL) and diethyl ether (25 mL) and dried *in vacuo*. White solid **13a** was obtained in 50% yield. ^{1}H NMR (300 MHz, CD_3OD, 25 °C): δ = 2.84 (s, 12H, NC*H*$_3$); 3.96 (s, 4H, C*H*$_2$N); 6.32 (s, 2H, Ar*H*). ^{13}C NMR (75.5 MHz, CD_3OD, 25 °C): δ = 53.19 (NCH$_3$); 75.35 (*C*H$_2$N); 108.27, 145.06, 146.98, 156.72 (Ar*C*). Anal. Calc. for $C_{12}H_{19}ClN_2OPd$ (349.16): C, 41.28; H, 5.48; N, 8.02. Found: C, 41.28; H, 5.59; N, 7.95%.

4.8. Synthesis of [Pd{$OC_6H_2(CH_2NMe_2)_2$-3,5-(PdI)-4}{$C_6H_2(CH_2NMe_2)_2$-2,6-(OH)-4}] (**15**)

[PdI{$C_6H_2(CH_2NMe_2)_2$-2,6-(*t*-BuMe$_2$SiO)-4}] (**11b**, 0.9 mmol) was dissolved in THF (20 mL). Tetrabutylammonium fluoride (1 mmol, 1 mL of 1 M solution in THF) was added to this solution. The solution turned turbid and then became clear. The resulting reaction mixture was stirred for 1 h. It became turbid again during this time. THF was evaporated and the product was washed with water, acetone and ether, and dried *in vacuo*. Compound **15** was obtained as a yellow colored powder. ^{1}H NMR (300 MHz, CD_2Cl_2, 25 °C): δ = 2.70, 2.96 (s, 24H, NC*H*$_3$); 3.84, 3.88 (s, 8H, NC*H*$_2$); 6.55, 6.61 (Ar*H*, 4H). ^{1}H NMR (300 MHz, $(CD_3)_2SO$, 25 °C): δ = 2.75 (s, 24H, NC*H*$_3$); 3.83 (s, 8H, NC*H*$_2$); 6.10 (Ar*H*, 4H). ^{13}C NMR (75.5 MHz, $(CD_3)_2SO$, 25 °C): δ = 52.52 (NCH$_3$); 73.84 (NCH$_2$); 107.16, 144.94, 145.94, 154.44 (Ar*C*). Anal. Calc. for $C_{24}H_{37}IN_4O_2Pd_2$ (753.32): C, 38.26; H, 4.95; I, 16.85; N, 7.44. Found: C, 38.18; H 5.06; I 16.72; N 7.38%.

4.9. Synthesis of [PdI{$C_6H_2(CH_2NMe_2)_2$-2,6-(OH)-4}] (**13b**)

Compound **15** (100 mg, 0.133 mmol) was treated with ammonium iodide (21 mg, 0.146 mmol) in methanol (10 mL). A white precipitate formed which was allowed to settle down. The supernatant yellowish solution was separated and residue was washed with methanol (2 × 5 mL). The combined washings and supernatant were subjected to vacuum. Compound **13b** was obtained as a white powder in 80% yield. ^{1}H NMR (300 MHz, CD_2Cl_2, 25 °C): 2.97 (s, 12H, NCH_3); 3.94 (s, 4H, NCH_2); 6.32 (Ar*H*, 2H). Anal. Calc. for $C_{12}H_{19}IN_2OPd$ (440.62): C, 32.71; H, 4.35; I 28.80; N, 6.36. Found: C, 32.62; H 4.28; I 28.74; N 6.27%.

4.10. Synthesis of [PdCl{$C_6H_2(CH_2NMe_2)_2$-2,6-((EtO)$_3$Si$(CH_2)_3$NHC(O)O)-4}] (**16**)

Triethoxysilylpropyl isocyanate (0.54 g, 2.2 mmol) was added to a solution of **13a** (0.7 g, 2 mmol), triethylamine (0.22 g, 2.2 mmol), and 4-(dimethylamino)pyridine (27 mg, 0.1 mmol) in dry dichloromethane (15 mL). The resulting reaction mixture was refluxed for 16 h after which a clear yellowish colored solution had formed. After allowing the reaction mixture to attain room temperature, all volatiles were removed *in vacuo*. The residue was washed with pentane (2 × 15 mL). The product was extracted from the residue by treating it with benzene (3 × 15 mL). The combined extracts were filtered to remove insoluble impurities and the solvent was evaporated *in vacuo* to obtain **16** as a yellowish solid in more than 90% yield. ^{1}H NMR (300 MHz, C_6D_6, 25 °C): δ = 0.68 (t, $^3J_{H,H}$ = 8.4 Hz, 2H, SiCH_2); 1.16 (t, $^3J_{H,H}$ = 6.9 Hz, 9H, OCH$_2$CH_3); 1.81 (quin, $^3J_{H,H}$ = 7.6 Hz, 2H, CH_2); 2.63 (s, 12H, NCH_3); 3.28 (quart, $^3J_{H,H}$ = 6.6 Hz, 2H, NHCH_2); 3.30 (s, 4H, CH_2N); 3.77 (quart, $^3J_{H,H}$ = 6.9 Hz, 6H, OCH_2); 6.11 (t, $^3J_{H,H}$ = 6.0 Hz, 1H, N*H*); 6.62 (s, 2H, Ar*H*). ^{13}C NMR (50 MHz, C_6D_6, 25 °C): δ = 8.67 (SiCH$_2$); 19.02 (OCH$_2$CH_3); 24.31 (CH_2); 44.51 (NHCH_2); 53.22 (NCH_3); 58.96 (OCH_2); 74.90 (CH_2N); 114.36 (*m*-C Ar), 146.13 (*ipso*-C Ar), 150.01 (*o*-C Ar), 153.61 (*p*-C Ar); 155.60 (*C*=O). ^{29}Si NMR (59.6 MHz, C_6D_6, 25 °C, TMS as reference): δ = −45.7. IR (ATR): $\tilde{\nu}$ (cm^{-1}) = 731 (N–H wag); 956 (sym Si–O–C stretching); 1100–1074 (asym. Si–O–C stretching, doublet); 1228 (C–N stretching); 1440 (N–H bending); 1520 (CHN group); 1730 (C=O stretching); 2887, 2926, 2975 (C–H stretching); 3313 (N–H stretching, associated). Anal. Calc. for $C_{22}H_{40}ClN_3O_5PdSi$ (596.53): C, 44.30; H, 6.76; N, 7.04; Si, 4.71. Found: C, 44.46; H, 6.81; N, 7.11; Si, 4.75%.

4.11. Synthesis of [PtI{$C_6H_2(CH_2NMe_2)_2$-2,6-((EtO)$_3$Si$(CH_2)_3$NHC(O)O)-4}] (**17**)

For the synthesis of this complex, a similar procedure was followed as described above for **16**. Using 0.75 g (1.42 mmol) of **14b**, compound **17** was isolated in 90% yield. ^{1}H NMR (200 MHz, C_6D_6, 25 °C): δ = 0.67 (t, $^3J_{H,H}$ = 8.8 Hz, 2H, SiCH_2); 1.17 (t, $^3J_{H,H}$ = 7.0 Hz, 9H, OCH$_2$CH_3); 1.79 (quin, $^3J_{H,H}$ = 7.6 Hz, 2H, CH_2); 2.75 (t, $^3J_{H,Pt}$ = 16.0 Hz, 12H, NCH_3); 3.28 (quart, $^3J_{H,H}$ = 6.6 Hz, 2H, NHCH_2); 3.36 (t, $^3J_{H,Pt}$ = 21.2 Hz, 4H, CH_2N); 3.78 (quart, $^3J_{H,H}$ = 7.0 Hz, 6H, OCH_2); 5.87 (t, $^3J_{H,H}$ = 6.2 Hz, 1H, N*H*); 6.69 (s, 2H, Ar*H*). ^{13}C NMR (50 MHz, C_6D_6, 25 °C): δ = 8.63 (SiCH$_2$); 19.01 (OCH$_2$CH_3); 24.29 (CH_2); 44.47 (NHCH_2); 54.48 (NCH_3); 58.95 (OCH_2); 77.83 (CH_2N); 114.04 (*m*-C Ar), 143.29 (*ipso*-C Ar), 144.47 (*o*-C Ar), 149.04 (*p*-C Ar), 155.60 (*C*=O). IR (ATR): $\tilde{\nu}$ (cm^{-1}) = 765 (N–H wag); 945 (sym Si–O–C stretching); 1100–1073 (asym. Si–O–C stretching, doublet); 1232 (C–N stretching); 1441 (N–H bending); 1522 (CHN group); 1712 (C=O stretching); 2888, 2924, 2973 (C–H stretching); 3284, 3340 (N–H stretching, associated).

4.12. Synthesis of [PdCl{$C_6H_2(CH_2PPh_2)_2$-2,6-((EtO)$_3$Si$(CH_2)_3$NHCOO)-4}] (**18**)

For the synthesis of this complex, a similar procedure was followed as described above for **16**. Using 0.2 g (0.317 mmol) of **8**, compound **18** was isolated in quantitative yield. ^{1}H NMR (300 MHz, C_6D_6, 25 °C): δ = 0.65 (t, $^3J_{H,H}$ = 7.95 Hz, 2H, SiCH_2); 1.17 (t, $^3J_{H,H}$ = 7.14 Hz, 9H, OCH$_2$CH_3); 1.73 (quin, $^3J_{H,H}$ = 7.68 Hz, 2H, CH_2); 3.21 (quart, $^3J_{H,H}$ = 6.33 Hz, 2H, NHCH_2); 3.47 (vt, $^2J_{H,P}$ = 4.5 Hz, 4H, PCH_2); 3.78 (quart, $^3J_{H,H}$ = 6.1 Hz, 6H, OCH_2); 5.47 (t, $^3J_{H,H}$ = 5.8 Hz, 1H, N*H*); 7.06 (s, 2H, Ar*H*); 6.9–7.0 (m, 12H, Ph*H*); 7.9–8.0 (m, 8H, Ph*H*). ^{13}C NMR (75.5 MHz, C_6D_6, 25 °C): δ = 8.17 (SiCH$_2$); 18.55 (OCH$_2$CH$_3$); 23.76 (CH$_2$); 42.51 (vt, $^1J_{C,P}$ = 14.7 Hz, CH$_2$P); 43.95 (NHCH$_2$); 58.56 (OCH$_2$); 116.92 (vt, $^3J_{C,P}$ = 12.0 Hz, *m*-C Ar), 128.84 (vt, $^3J_{C,P}$ = 5.5 Hz, *m*-C Ph), 130.48 (*p*-C Ph), 132.90 (vt, $^1J_{C,P}$ = 21.8 Hz, *ipso*-C Ph), 133.34 (vt, $^2J_{C,P}$ = 7.1 Hz, *o*-C Ph), 149.27 (vt, $^2J_{C,P}$ = 11.4 Hz, *ipso*-C Ar), 150.56 (*o*-C Ar), 154.78 (*p*-C Ar); 157.0 (*C*=O). ^{31}P NMR (81 MHz, C_6D_6, 25 °C): δ = 33.4. IR (ATR): $\tilde{\nu}$ (cm^{-1}) = 740 (N–H wag); 955 (sym Si–O–C stretching); 1100–1071 (asym. Si–O–C stretching, doublet); 1227 (C–N stretching); 1435 (N–H bending); 1513 (CHN group); 1734 (C=O stretching); 2886, 2926, 2973, 3052 (C–H stretching); 3314 (N–H stretching, associated). Anal. Calc. for $C_{42}H_{48}ClNO_5P_2PdSi$ (878.74): C, 57.41; H, 5.51; N, 1.59; P, 7.05. Found: C, 57.54; H, 5.46; N, 1.53; P, 7.02%.

4.13. Synthesis of [PdBr{$C_6H_2(CH_2SPh)_2$-2,6-((EtO)$_3$Si$(CH_2)_3$NHCOO)-4}] (**19**)

For the synthesis of this complex, a similar procedure was followed as described above for **16**. Using 0.2 g (0.38 mmol) of **9b**, compound **19** was isolated in quantitative yield. ^{1}H NMR (300 MHz, $CDCl_3$, 25 °C): δ = 0.63 (t, $^3J_{H,H}$ = 8.1 Hz, 2H, SiCH_2); 1.20 (t, $^3J_{H,H}$ = 6.9 Hz, 9H, OCH$_2$CH_3); 1.65 (quin, $^3J_{H,H}$ = 6.9, 7.8 Hz, 2H, CH_2); 3.19 (quart, $^3J_{H,H}$ = 6.3 Hz, 2H, NHCH_2); 3.80 (quart, $^3J_{H,H}$ = 6.9 Hz, 6H, OCH_2); 4.51 (s, 4H, SCH_2); 5.52 (t, $^3J_{H,H}$ = 5.5 Hz, 1H, N*H*); 6.74 (s, 2H, Ar*H*); 7.31–7.33 (m, 6H, Ph*H*); 7.76–7.79 (m, 4H, Ph*H*). ^{13}C NMR (75.5 MHz, $CDCl_3$, 25 °C): δ = 7.72 (SiCH$_2$); 18.31 (OCH$_2$CH$_3$); 23.06 (CH$_2$); 40.96 (NHCH$_2$); 51.53 (SCH$_2$); 58.50 (OCH$_2$); 115.75 (*m*-C Ar), 129.68 (*o*-C Ph), 129.88 (*p*-C Ph), 131.44 (*m*-C PhS), 132.19 (*ipso*-C Ph), 148.75 (*ipso*-C Ar), 150 (*o*-C Ar), 154.54 (*p*-C Ar); 156.91 (*C*=O). ^{29}Si NMR (59.6 MHz, $CDCl_3$, 25 °C): δ = −45.85. IR (ATR): $\tilde{\nu}$ (cm^{-1}) = 742 (N–H wag); 953 (sym Si–O–C stretching); 1100–1074 (asym. Si–O–C stretching, doublet); 1221 (C–N stretching); 1441 (N–H bending); 1519 (CHN group); 1731 (C=O stretching); 2885, 2926, 2973 (C–H stretching); 3302 (N–H stretching, associated). Anal. Calc. for $C_{30}H_{38}BrNO_5PdS_2Si$ (771.17): C, 46.72; H, 4.97; N, 1.82; S, 8.32. Found: C, 46.11; H, 4.71; N, 1.94; S, 8.43%.

4.14. X-ray crystal structure determinations

X-ray intensities were measured on a Nonius KappaCCD diffractometer with rotating anode and graphite monochromator (λ = 0.71073 Å) at a temperature of 150 K up to a resolution of $(\sin\theta/\lambda)_{max}$ = 0.65 Å^{-1}. The structures were solved with automated Patterson Methods (DIRDIF-99 [42] for **6**, **9a**, **15**, and **17**). The starting coordinates for **13a** were taken from the isostructural Pt compound. Refinement was performed with SHELXL-97 [43] against F^2 of all reflections. Thereby non-hydrogen atoms were refined freely with anisotropic displacement parameters. Geometry calculations and checking for higher symmetry were performed with the PLATON [44] program. In **9a** and **13a**, all hydrogen atoms were located in the Difference Fourier map. The OH hydrogen atom was refined freely with isotropic displacement parameters. All other hydrogen atoms were refined with a riding model. In **6** and **17**, all hydrogen

atoms were introduced in calculated positions and refined with a riding model. The crystal structure of **6** was refined as a pseudo-orthorhombic twin with a twofold rotation about the reciprocal c^* axis as twin operation. The twin fraction refined to 0.4315(5). In **15**, the OH hydrogen atoms were located in the Difference Fourier map and kept fixed in their located positions. All other hydrogen atoms were introduced in calculated positions and refined with a riding model. One methanol was refined with full occupancy, the second methanol with a partial occupancy of 2/3. Further crystallographic details are given in Supplementary material, Table S1.

Acknowledgements

This work was supported in part by the Dutch Technology Foundation STW, Utrecht University (N.C.M.) and by the Council for Chemical Sciences of the Netherlands Organization for Scientific Research (CW-NWO; M.L. and A.L.S.). R.J.M.K.G. thanks the National Research School Combination Catalysis (NRSC-C) for financial support.

Appendix A. Supplementary material

CCDC 683861, 683863, 683863, 683864 and 683865 contain the supplementary crystallographic data for **6**, **9a**, **13a**, **15** and **17**. These data can be obtained free of charge from The Cambridge Crystallographic Data Centre via www.ccdc.cam.ac.uk/data_request/cif. Experimental details for the X-ray crystal structure determinations of **6**, **9a**, **13a**, **15** and **17**. Supplementary data associated with this article can be found, in the online version, at doi:10.1016/j.jorganchem.2008.06.016.

References

[1] D.E. Bergbreiter, J.D. Frels, J. Rawson, J. Li, J.H. Reibenspies, Inorg. Chim. Acta 359 (2006) 1912;
A.V. Chuchuryukin, H.P. Dijkstra, B.M.J.M. Suijkerbuijk, R.J.M. Klein Gebbink, G.P.M. van Klink, A.M. Mills, A.L. Spek, G. van Koten, Angew. Chem., Int. Ed. 42 (2003) 228;
H.P. Dijkstra, M.D. Meijer, J. Patel, R. Kreiter, G.P.M. van Klink, M. Lutz, A.L. Spek, A.J. Canty, G. van Koten, Organometallics 20 (2001) 3159;
P. Dani, B. Richter, G.P.M. van Klink, G. van Koten, Eur. J. Inorg. Chem. (2001) 125;
S. Back, R.A. Gossage, H. Lang, G. van Koten, Eur. J. Inorg. Chem. (2000) 1457.
[2] H.P. Dijkstra, M.Q. Slagt, A. McDonald, C.A. Kruithof, R. Kreiter, A.M. Mills, M. Lutz, A.L. Spek, W. Klopper, G.P.M. van Klink, G. van Koten, Eur. J. Inorg. Chem. (2003) 830.
[3] D.E. Bergbreiter, P.L. Osburn, J.D. Frels, J. Am. Chem. Soc. 123 (2001) 11105.
[4] S. Back, M. Albrecht, A.L. Spek, G. Rheinwald, H. Lang, G. van Koten, Organometallics 20 (2001) 1024.
[5] M. Albrecht, G. van Koten, Angew. Chem., Int. Ed. 40 (2001) 3750.
[6] M. Albrecht, G. Rodriguez, J. Schoenmaker, G. van Koten, Org. Lett. 2 (2000) 3461.
[7] W.T.S. Huck, B. Snellink-Ruël, F.C.J.M. van Veggel, D.N. Reinhoudt, Organometallics 16 (1997) 4287.
[8] P.J. Davies, N. Veldman, D.M. Grove, A.L. Spek, B.T.G. Lutz, G. van Koten, Angew. Chem., Int. Ed. 35 (1996) 1959.
[9] W.T.S. Huck, F.C.J.M. van Veggel, B.L. Kropman, D.H.A. Blank, E.G. Keim, M.M.A. Smithers, D.N. Reinhoudt, J. Am. Chem. Soc. 117 (1995) 8293.
[10] M.Q. Slagt, G. Rodriguez, M.M.P. Grutters, R.J.M. Klein Gebbink, W. Klopper, L.W. Jenneskens, M. Lutz, A.L. Spek, G. van Koten, Chem. Eur. J. 10 (2004) 1331.
[11] R.A. Gossage, L.A. van de Kuil, G. van Koten, Acc. Chem. Res. 31 (1998) 423.
[12] I. Goettker-Schnetmann, P.S. White, M. Brookhart, Organometallics 23 (2004) 1766.
[13] D.E. Bergbreiter, S. Furyk, Green Chem. 6 (2004) 280.
[14] M.Q. Slagt, J.T.B.H. Jastrzebski, R.J.M. Klein Gebbink, H.J. van Ramesdonk, J.W. Verhoeven, D.D. Ellis, A.L. Spek, G. van Koten, Eur. J. Org. Chem. (2003) 1692.
[15] D.E. Bergbreiter, P.L. Osburn, Y.-S. Liu, J. Am. Chem. Soc. 121 (1999) 9531.
[16] N.C. Mehendale, J.R.A. Sietsma, K.P. de Jong, C.A. van Walree, R.J.M. Klein Gebbink, G. van Koten, Adv. Synth. Catal. 349 (2007) 2619.
[17] N.C. Mehendale, C. Bezemer, C.A. van Walree, R.J.M. Klein Gebbink, G. van Koten, J. Mol. Catal. A 257 (2006) 167.
[18] R. Gimenez, T.M. Swager, J. Mol. Catal. A 166 (2001) 265;
R. Chanthateyanonth, H. Alper, J. Mol. Catal. A 201 (2003) 23;
R. Chanthateyanonth, H. Alper, Adv. Synth. Catal. 346 (2004) 1375.
[19] H.P. Dijkstra, N. Ronde, G.P.M. van Klink, D. Vogt, G. van Koten, Adv. Synth. Catal. 345 (2003) 364;
H.P. Dijkstra, C.A. Kruithof, N. Ronde, R. van de Coevering, D.J. Ramón, D. Vogt, G.P.M. van Klink, G. van Koten, J. Org. Chem. 68 (2003) 675.
[20] G. Rodriguez, M. Lutz, A.L. Spek, G. van Koten, Chem. Eur. J. 8 (2002) 45;
C. Schlenk, A.W. Kleij, H. Frey, G. van Koten, Angew. Chem., Int. Ed. 39 (2000) 3445.
[21] M.D. Meijer, B. Mulder, G.P.M. van Klink, G. van Koten, Inorg. Chim. Acta 352 (2003) 247;
M.D. Meijer, N. Ronde, D. Vogt, G.P.M. van Klink, G. van Koten, Organometallics 20 (2001) 3993.
[22] G. Guillena, G. Rodriguez, M. Albrecht, G. van Koten, Chem. Eur. J. 8 (2002) 5368.
[23] C.A. Kruithof, M.A. Casado, G. Guillena, M.R. Egmond, A. van der Kerk-van Hoof, A.J.R. Heck, R.J.M. Klein Gebbink, G. van Koten, Chem. Eur. J. 11 (2005) 6869.
[24] M. Gagliardo, D.J.M. Snelders, P.A. Chase, R.J.M. Klein Gebbink, G.P.M. van Klink, G. van Koten, Angew. Chem., Int. Ed. 46 (2007) 8558.
[25] C.R. South, M.N. Higley, K.C.F. Leung, D. Lanari, A. Nelson, R.H. Grubbs, J.F. Stoddart, M. Weck, Chem. Eur. J. 12 (2006) 3789;
J.M. Pollino, M. Weck, Chem. Soc. Rev. 34 (2005) 193;
H. Hofmeier, U.S. Schubert, Chem. Commun. (2005) 2423;
W.C. Yount, D.M. Loveless, S.L. Craig, Angew. Chem., Int. Ed. 44 (2005) 2746;
J.M. Pollino, L.P. Stubbs, M. Weck, J. Am. Chem. Soc. 126 (2004) 563;
W.C. Yount, H. Juwarker, S.L. Craig, J. Am. Chem. Soc. 125 (2003) 15302.
[26] M.Q. Slagt, H.P. Dijkstra, A. McDonald, R.J.M. Klein Gebbink, M. Lutz, D.D. Ellis, A.M. Mills, A.L. Spek, G. van Koten, Organometallics 22 (2003) 27;
S.J. Loeb, G.K.H. Shimizu, J. Chem. Soc., Chem. Commun. (1993) 1395.
[27] M. Albrecht, M. Lutz, A.M.M. Schreurs, E.T.H. Lutz, A.L. Spek, G. van Koten, J. Chem. Soc., Dalton Trans. (2000) 3797.
[28] M. Albrecht, R.A. Gossage, M. Lutz, A.L. Spek, G. van Koten, Chem. Eur. J. 6 (2000) 1431.
[29] S.L. James, G. Verspui, A.L. Spek, G. van Koten, Chem. Commun. (1996) 1309.
[30] M. Albrecht, M. Lutz, A.L. Spek, G. van Koten, Nature 406 (2000) 970.
[31] M. Gagliardo, N. Selander, N.C. Mehendale, G. van Koten, R.J.M. Klein Gebbink, K.J. Szabó, Chem. Eur. J. 14 (2008) 4800;
K.J. Szabó, Synlett (2006) 811;
S. Sebelius, V.J. Olsson, K.J. Szabó, J. Am. Chem. Soc. 127 (2005) 10478;
J. Kjellgren, J. Aydin, O.A. Wallner, I.V. Saltanova, K.J. Szabó, Chem. Eur. J. 11 (2005) 5260;
J. Kjellgren, H. Sunden, K.J. Szabó, J. Am. Chem. Soc. 127 (2005) 1787;
O.A. Wallner, K.J. Szabó, J. Org. Chem. 70 (2005) 9215;
J. Zhao, A.S. Goldman, J.F. Hartwig, Science 307 (2005) 1080;
O.A. Wallner, K.J. Szabó, Org. Lett. 6 (2004) 1829;
N. Solin, O.A. Wallner, K.J. Szabó, Org. Lett. 7 (2005) 689;
N. Solin, J. Kjellgren, K.J. Szabó, J. Am. Chem. Soc. 126 (2004) 7026;
J. Kjellgren, H. Sunden, K.J. Szabó, J. Am. Chem. Soc. 126 (2004) 474;
K. Takenaka, Y. Uozumi, Org. Lett. 6 (2004) 1833;
J.S. Fossey, C.J. Richards, Organometallics 23 (2004) 367;
Z. Wang, M.R. Eberhard, C.M. Jensen, S. Matsukawa, Y. Yamamoto, J. Organomet. Chem. 681 (2003) 189;
E. Diez-Barra, J. Guerra, V. Hornillos, S. Merino, J. Tejeda, Organometallics 22 (2003) 4610;
J.T. Singleton, Tetrahedron 59 (2003) 1837;
M.E. van der Boom, D. Milstein, Chem. Rev. 103 (2003) 1759;
G.R. Rosa, G. Ebeling, J. Dupont, A.L. Monteiro, Synthesis (2003) 2894;
I.G. Jung, S.U. Son, K.H. Park, K.-C. Chung, J.W. Lee, Y.K. Chung, Organometallics 22 (2003) 4715;
J.S. Fossey, C.J. Richards, Tetrahedron Lett. 44 (2003) 8773;
S. Sjoevall, O.F. Wendt, C. Andersson, J. Chem. Soc., Dalton Trans. (2002) 1396;
J.M. Seul, S. Park, J. Chem. Soc., Dalton Trans. (2002) 1153;
D. Morales-Morales, R.E. Cramer, C.M. Jensen, J. Organomet. Chem. 654 (2002) 44;
J.A. Loch, M. Albrecht, E. Peris, J. Mata, J.W. Faller, R.H. Crabtree, Organometallics 21 (2002) 700;
B.S. Williams, P. Dani, M. Lutz, A.L. Spek, G. van Koten, Helv. Chim. Acta 84 (2001) 3519;
S. Gruendemann, M. Albrecht, J.A. Loch, J.W. Faller, R.H. Crabtree, Organometallics 20 (2001) 5485;
J. Dupont, M. Pfeffer, J. Spencer, Eur. J. Inorg. Chem. (2001) 1917;
D. Morales-Morales, C. Grause, K. Kasaoka, R. Redon, R.E. Cramer, C.M. Jensen, Inorg. Chim. Acta 300–302 (2000) 958;
D. Morales-Morales, R. Redon, C. Yung, C.M. Jensen, Chem. Commun. (2000) 1619;
M.A. Stark, G. Jones, C.J. Richards, Organometallics 19 (2000) 1282;
R.A. Gossage, J.T.B.H. Jastrzebski, J. van Ameijde, S.J.E. Mulders, A.J. Brouwer, R.M.J. Liskamp, G. van Koten, Tetrahedron Lett. 40 (1999) 1413;
X. Zhang, J.M. Longmire, M. Shang, Organometallics 17 (1998) 4374;
M. Ohff, A. Ohff, M.E. van der Boom, D. Milstein, J. Am. Chem. Soc. 119 (1997) 11687;
S.E. Denmark, R.A. Stavenger, A.-M. Faucher, J.P. Edwards, J. Org. Chem. 62 (1997) 3375;
F. Gorla, A. Togni, L.M. Venanzi, A. Albinati, F. Lianza, Organometallics 13 (1994) 1607.
[32] R. Chauvin, Eur. J. Inorg. Chem. (2000) 577.
[33] P.J. Davies, D.M. Grove, G. van Koten, Organometallics 16 (1997) 800.

[34] J.-M. Valk, R. van Belzen, J. Boersma, A.L. Spek, G. van Koten, J. Chem. Soc., Dalton Trans. (1994) 2293;
J.-M. Valk, J. Boersma, G. van Koten, J. Organomet. Chem. 483 (1994) 213;
P.L. Alsters, P.F. Engel, M.P. Hogerheide, M. Copijn, A.L. Spek, G. van Koten, Organometallics 12 (1993) 1831.
[35] P. Steen winkel, S.L. James, D.M. Grove, H. Kooijman, A.L. Spek, G. van Koten, Organometallics 16 (1997) 513;
P. Steenwinkel, J.T.B.H. Jastrzebski, B.-J. Deelman, D.M. Grove, H. Kooijman, N. Veldman, W.J.J. Smeets, A.L. Spek, G. van Koten, Organometallics 16 (1997) 5486.
[36] P.L. Alsters, P.J. Baesjou, M.D. Janssen, H. Kooijman, A. Sicherer-Roetman, A.L. Spek, G. van Koten, Organometallics 11 (1992) 4124.
[37] G.M. Kapteijn, M.D. Meijer, D.M. Grove, N. Veldman, A.L. Spek, G. van Koten, Inorg. Chim. Acta 264 (1997) 211.
[38] G.M. Kapteijn, D.M. Grove, H. Kooijman, W.J.J. Smeets, A.L. Spek, G. van Koten, Inorg. Chem. 35 (1996) 526.
[39] Excellent solubility properties are important to achieve uniform distribution of the catalyst on the support.
[40] D. Braga, F. Grepioni, G.R. Desiraju, Chem. Rev. 98 (1998) 1375.
[41] W.T.S. Huck, F.C.J.M. van Veggel, D.N. Reinhoudt, J. Mater. Chem. 7 (1997) 1213.
[42] P.T. Beurskens, G. Admiraal, G. Beurskens, W.P. Bosman, S. Garcia-Granda, R.O. Gould, J.M.M. Smits, C. Smykalla, The DIRDIF99 program system, Technical Report of the Crystallography Laboratory, University of Nijmegen, The Netherlands, 1999.
[43] G.M. Sheldrick, SHELXL-97 Program for crystal structure refinement, Universität Göttingen, Germany, 1997.
[44] A.L. Spek, J. Appl. Crystallogr. 36 (2003) 7.